Analysis of Energy Harvesting for Vibration-Motivated Wireless Sensor Networks

Sunho Lim
Dept. of Computer Science
Texas Tech University
Lubbock, TX 79409
sunho.lim@ttu.edu

Jung-Han Kimn
Dept. of Mathematics and Statistics
South Dakota State University
Brookings, SD 57007
jung-han.kimn@sdstate.edu

Hyeoungwoo Kim
Advanced Cerametrics, Inc.
Lambertville, NJ 08530
hyeoungwookim@advanced-cerametrics.com

***Abstract*—**
Extracting an electrical energy from various environmental sources, called energy harvesting (or energy scavenging), has been attracting researchers' attention in energy replenishable networks. In particular, a piezoelectric device based energy harvesting from ambient vibrations is a promising technique for easy of battery energy replenishment in vibration-motivated wireless sensor networks (WSNs). In this paper, we address two major issues of vibration-based energy harvesting: impact spread and energy conversion. A simple analytical model of the impact spread is proposed to estimate the impact over time and distance, in which diffusion equation is used for easy of analysis. Then we propose a modified inverse Bézier curve method for an explicit interpolation function to support a seamless energy conversion. The overall analyses and numerical results indicate that the proposed techniques are proven to be a viable approach for analyzing vibration-motivated WSNs.

***Index Terms*—Energy harvesting, Piezoelectric transducer, Vibration, Wireless sensor networks.**

I. Introduction

A wireless sensor network (WSN) consists of a large number of small devices (later nodes) equipped with sensing, computing, and communicating facilities [1]. Recent technological advances have fueled the development of a tiny, low-cost, and low-power node which is applicable to a wide range of applications for WSNs. For example, WSNs have been integrated with structural health monitoring systems [2], [3] that are designed to detect and locate the structural damages occurred in such as bridges, buildings, dams, ships, aircrafts, etc. Each node equipped with a vibration detecting card can be installed in a structure. Then it continuously monitors a structural state by measuring ambient vibrations caused by passing vehicles [2] or trains [3]. We envision that WSN and its technology will be penetrated into our daily life and become a ubiquitous communication infrastructure in the near future.

However, due to a limited amount of battery energy, there has been a great deal of research efforts on the developing various energy aware techniques in the WSNs. Particularly in routing, each node plays a role as either a sensed data sender or a router. Thus, it is essential to judiciously reduce the energy spent for communication activities (e.g. transmission, reception, and forwarding) without degrading the communication performance such as a network lifetime. Also since nodes are usually required to operate for a long period of time in an unattended environment, it is inconvenient or hard (if it is not impossible) to either replace or replenish the battery.

In light on this, researchers in the academy and industry have been focused on the extracting an electrical energy from various environmental sources, called *energy harvesting* (or *energy scavenging*), for easy of battery energy replenishment. The environmental sources include vibrations, magnetic fields, thermal gradients, lights, kinetic motions, shock waves, etc. They motivate to generate an electrical energy through the combination with available components including piezoelectric, magnetoelectric, thermoelectric, and semiconductor, in which all these components have inherent pros and cons. When vibrations are a dominant source of energy and solar light is not always available, it has been found that piezoelectric-based energy harvesting is the most promising technique [4]. Here, vibrations can be generated in various places such as rotating machineries or engines, bridges due to passing vehicles or trains, buildings or dams due to wind or flowing water, etc.

In this paper, we analyze a piezoelectric device based energy harvesting from vibrations, and address two major issues for vibration-motivated WSNs: impact spread and energy conversion. Our contributions are two folds:

- First, we develop a simple analytical model for the impact spread to facilitate the estimation of impact over time and distance, in which diffusion equation is used for easy of analysis. The impact spread is simulated and observed in terms of either single or multiple impact sources.
- Second, we propose a modified inverse Béizer curve technique for an explicit interpolation function to support a seamless energy conversion. The proposed interpolation function is easily implementable under low computational complexity and overhead.

The rest of paper is organized as follows. The prior work is carefully reviewed and analyzed in Section II. A simple analytical model of impact spread and an energy interpolation function are presented in Sections III and IV, respectively. Section V presents our numerical results. Finally, we conclude the paper with future directions in Section VI.

II. Related Work

Harvesting energy from ambient vibrations using a piezoelectric transducer has been investigated and applied to the wide range of applications [5], [6], [7], [8]. Hausler *et al* [5] proposed the implantation of piezoelectric polymer patches into a living body to harvest energy from breathing. Body heat, blood pressure, and breath pressure have a potential for generating electric energy. In [6], piezoelectric materials are used in the soles of shoes, where an electrical power is generated through walking. Researchers also have demonstrated the possibility of embedding a piezoelectric component in a textile [7]. In addition, mechanical flow energy in oceans and rivers is utilized to convert electrical energy by using piezoelectric polymer actuators [8]. They can provide a large amount of electrical power levels because of the vast size of the flowing water resource.

WSNs have been integrated with various energy harvesting systems, especially in structural health monitoring systems [9], [2], [3]. The monitoring system is designed to detect and locate the structural damages occurred in various places. Traditional hardwired nodes can be deployed instead, but they incur the high cost of wiring and long setup delay. Thus, they limits the location where the nodes can be installed [9]. In addition, the maintenance cost including both locating and replacing the batteries becomes non-negligible. It is because of the frequent measurements of ambient vibrations and non-homogeneous energy consumption.

A number of recent studies have been conducted with a set of re-chargeable nodes in WSNs [10], [11], [12], [13], [14], [15]. Here, each node's battery is replenished by energy harvesting from various environmental sources [16], [11], [10], [17], [18], [4]. In [11], [14], a solar-based energy harvesting model is presented and it is applied to scheduling and routing methodologies. They shown that the proposed energy harvesting aware routing can increase a network lifetime compared to that of traditional battery aware routing schemes. Kar *et al.* [12] proposed several threshold policies to maximize the communication performance by activating the node dynamically. Each node's battery is assumed to be randomly recharged and it changes its state into one of three states such as active, passive, or ready. Voigt *et al.* [10] proposed a solar aware routing, in which a packet is forwarded to the node powered by the solar energy.

Although there may exist many energy harvesting techniques in WSNs, little effort has been devoted in exploring the analytical models of impact spread and energy interpolation function in vibration-motivated WSNs.

III. A Simple Model of Impact Spread

In this section, we first present a simple analytical model of impact spread based on diffusion equation[1]. Then we analyze the impact spread depending on either single or multiple impact sources.

[1]The detail description about the mathematical properties and physical meaning of the diffusion equation can be found in [19], [20].

A. The Impact Spread

To build a simple analytical model of impact spread over time and distance, we consider an exponential normal distribution function. The impact spread function, $S(D,T)$, measures an amount of impact at time T and distance D, and it is expressed as,

$$S(D,T) = \frac{1}{(4\pi\kappa T)^{n/2}} e^{-|D|^2/4\kappa T}, \tag{1}$$

where n is the dimension of spatial domain. Also D and T are the distance and the impact spread time from the location of vibration source to the location where the impact is measured, respectively. In addition, κ is a proportionality factor which measures the rate of transferred energy from one location to another. To measure the impact from the node located in l at t, Eq. 1 can be rewritten as,

$$S(l-\xi, t-\tau) = \frac{1}{(4\pi\kappa(t-\tau))^{n/2}} e^{-|l-\xi|^2/4\kappa(t-\tau)}, \tag{2}$$

where ξ and τ are the impact location and its generation time, respectively. Here, $|l-\xi|$ is a distance[2]. Thus, we have $D = l-\xi$ and $T = t-\tau$, where T is always assumed positive (>0).

Eq. 2 is known as the fundamental solution of the diffusion equation expressed as,

$$u_t + \kappa\Delta u = \delta(l-\xi)\delta(t-\tau), \tag{3}$$

where δ is the Dirac delta function [20]. Eq. 3 is interpreted by the partial differential equation, which describes the behavior of flow with the concentrated unit source located in $l = \xi$ at time $t = \tau$. More precisely, it explains the movement of spread when the source turns on only the specific position ξ and instant τ without involving any other energy sources for entire (l,t), except (ξ,τ). Due to this *discrete* nature of the fundamental solution, Eq. 2 can be used to model an impact spread for a single impact source.

As a simple analytical model, we assume that the impact spread is like a conduction of fluid in a stationary medium. The spread of fluid model is based on Fick's law of diffusion[3] [20]. This model is formulated by diffusion equation expressed as,

$$u_t = \kappa\nabla\cdot\nabla u = \Delta u, \tag{4}$$

where $\Delta u = \frac{\partial^2 u}{\partial l_1^2} + \cdots + \frac{\partial^2 u}{\partial l_n^2}$. Δ is known as Laplace operator and expresses the physical law that does not depend on special location [19]. This operator also can be decomposed into $\Delta = \nabla\cdot(\nabla)$. Here, $\nabla\cdot$ and ∇ are divergence operator and gradient operator, respectively.

[2]This is a physical distance between two locations and is calculated by $\sqrt{\sum_{i=1}^{n}(l_i-\xi_i)^2}$.

[3]Fick's law states that the flux goes from the high concentration regions to the low concentration regions, and the rate of movement is proportional to the concentration gradient.

B. Single Source of Impact

We first consider a series of impacts generated at different times, in which each individual impact does not affect others. In this paper, we consider a two-dimensional spatial domain (n = 2), and thus Eq. 2 is reduced to,

$$S(l-\xi, t-\tau) = \frac{1}{4\pi\kappa(t-\tau)} e^{-|l-\xi|^2/4\kappa(t-\tau)}. \quad (5)$$

Then let us define an initial amount of impact in Eq. 5. Although function $S(l,t)$ is defined as the Dirac delta function (showing a very tall spike) for small t, the total energy of impact is calculated as below for the fixed t.

$$\int_{-\infty}^{\infty} S(l,t)\, dl = 1. \quad (6)$$

Let us define Eq. 6 as a unit of total impact. Then we can define the impact spread function with the Γ (> 0) amount of initial impact expressed as,

$$S_\Gamma(l-\xi, t-\tau) = \frac{\Gamma}{4\pi\kappa(t-\tau)} e^{-|l-\xi|^2/4\kappa(t-\tau)}. \quad (7)$$

Note that $S_\Gamma(D,T)$ with $D = l-\xi$ and $T = t-\tau$ has a fast decaying property with small T for any $D > 0$. Thus, in this paper, we use a scale correction parameter to gain a realistic value.

C. Multiple Sources of Impact

We now extend the impact spread function of Eq. 7 to consider a series of impacts generated at different times. Each individual impact is affected by prior impacts. Suppose we have m impacts generated at different locations $(\xi_1, \cdots, \xi_m)$ and times $(\tau_1, \cdots, \tau_m)$. We also assume different proportionality constants $(\kappa_1, \cdots, \kappa_m)$ and impacts $(\Gamma_1, \cdots, \Gamma_m)$. Then we can define the impact spread function for i^{th} impact by,

$$S_{\Gamma_i}(l-\xi_i, t-\tau_i) = \frac{\Gamma_i}{4\pi\kappa_i(t-\tau_i)} e^{-|l-\xi_i|^2/4\kappa(t-\tau_i)}. \quad (8)$$

For the purpose of combination of impacts, we assume $0 = \tau_1 \leq \tau_2 \leq \cdots \leq \tau_m$ without loss of generality. Then the total amount of impacts for i^{th} event is formulated as,

$$S(l,t) = \sum_{j=1}^{i} S_{\Gamma_j}. \quad (9)$$

In summary, we analyze the impact spread in terms of single and multiple impact sources based on diffusion equation. Since diffusion equation is one of the basic equations, we expect that our approach can be extended to meet more realistic physical phenomena. The extension can be formulated by adding more sophisticated differential equations and terms. Due to computational complexity and overhead, however, we do not consider the extended equation in this paper.

IV. Energy Conversion

In this section, we first briefly introduce a piezoelectric transducer for vibration-based energy harvesting. Then we present a Béizer curve based interpolation function to support a seamless energy conversion.

TABLE I
PROPERTIES OF PFCB-W14

Property	Value
Dimensions (mm)	132 × 14 × 1.3
Resonance frequency (Hz)	30±1
Bending stiffness (N/m)	56
Maximum bending displacement (mm)	50
Maximum voltage (V)	200

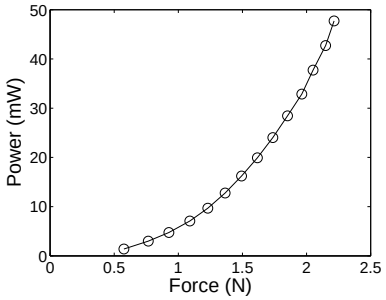

Fig. 1. The power generation against the impact force in PFCB-W14.

A. Piezoelectric Transducer

A piezoelectric transducer is a vibration-based energy harvester and primarily consists of a piezoelectric generator and a storage circuit. The conversion from mechanical energy to electrical energy is obtained through the direct piezoelectric effect in the generator, and the generated energy is stored in the storage circuit. The energy generation is directly related to the extent to which a ceramic element is deformed in the generator at the presence of impact, resulting in a vibration of the element. Thus, the configuration of the element and its manner of being mounted is an important factor to contribute the performance of the energy generation.

There are three steps of energy transformation in the piezoelectric generator. In the first step, the environmental energy source is trapped and transformed into the mechanical vibration energy of the piezoelectric transducer. As we aforementioned in Section III, the environmental energy can be generated in the form of either single or multiple events depending on whether each event is affected by prior event(s). In the second step, the mechanical vibration energy is transformed into the electrical energy, in which the direct piezoelectric effect is used. Finally, the generated electrical energy is stored and transferred to the output load for the application. In these transformations, there is a mechanical loss because of the mismatch in mechanical impedance represented by damping factor and reflection ratio. Also there is electro-mechanical loss depending upon the magnitude of electro-mechanical coupling factor [21]. Depending on the frequency and amplitude of the mechanical stress, one can design the required transducer, its dimensions, vibration mode, and desired piezoelectric material. Usually a piezoelectric ceramic element generates an electrical energy from a mechanical energy input. Under an ideally designed piezoelectric generator, electrical energy increases almost linearly with increasing mechanical energy.

In this paper, we use a piezoelectric fiber composite bi-

morph (PFCB) W14 as a piezoelectric component to trap an environmental energy and transform into a mechanical vibration energy. We summarize its properties in Tab. I. Base on the PFCB-W14, we can obtain a set of data points from an experimentation shown in Fig. 1.

B. Mapping Mechanical-to-Electrical Energy

To build a conversion function of mechanical-to-electrical energy, it is essential to approximate a new data point between known data points because of a limited number of data points obtained. In light on this, we consider an interpolation technique to generate a function that can estimate intermediate data points. Various alternatives [22] are existed depending on the constraints such as accuracy, complexity, and smoothness.

In order to develop an interpolation function based on a given original data set, we primarily focus on whether the function can generate a curve that is smooth and close enough to the original data set. Also the function should be simple enough so that it can easily control the shape of curve. However, interpolation techniques may generate a polynomial function, which can make a smooth curve but its overall shape can be deteriorated. In case of a lower order polynomial, it not only requires additional conditions but also incurs complicated formulas to make a smooth curve. Thus, although it is a conflict requirement, we should carefully select an interpolation technique that can generate a smooth curve and a simple formula with the less computational complexity and overhead.

In this paper, we consider a Bézier curve [22] based interpolation function to fulfill the aforementioned requirements. The Bézier curve is defined within interval $[0, 1]$ and formulated with the basic Bernstein polynomials $B_{(i,n)}$, $0 \leq i \leq n$. The polynomial $B_{(i,n)}$ is defined by,

$$B_{(i,n)}(t) = \begin{pmatrix} n \\ i \end{pmatrix} t^i (1-t)^{n-i}, \quad \begin{pmatrix} n \\ i \end{pmatrix} = \frac{n!}{i!(n-i)!}, \tag{10}$$

where $t \in [0, 1]$. For a continuous function f on $[0, 1]$, we can define the sequence of polynomials P_n, $n \geq 0$. The polynomial $P_n(t)$ is defined by,

$$P_n(t) = \sum_{i=0}^{n} f(\frac{i}{n}) B_{(i,n)}(t), \ t \in [0, 1].$$

Then P_n converges uniformly to f which implies,

$$\lim_{n \to \infty} \sup_{0 \leq t \leq 1} |f(t) - P_n(t)| = 0,$$

where $\sup$ means least upper bound of the given values. Thus, $P_n(t)$ converges to $f(t)$ with uniform rate of convergence on $[0, 1]$.

Also the set of polynomials $\{B_{(0,n)}, B_{(1,n)}, \cdots, B_{(n,n)}\}$ forms the basis for the vector space of all polynomial of degree not exceeding n. It means that any polynomial $P(t)$ in this vector space can be represented as,

$$P(t) = \sum_{i=0}^{n} B_{(i,n)}(t) A_i,$$

where A_i ($i = 0, \cdots, n$) are coefficients. The shape of curve can be changed by adjusting the coefficients, which are in fact the given data set. Thus, once the set of basis functions ($B_{(i,n)}$) for given n number of data set is defined, the Bézier curve is defined by using the data set as the coefficients. Then we can define the Bézier curve for 2-dimensional data set, $\{(x_i, y_i) | 0 \leq i \leq n\}$, expressed as,

$$x(t) = \sum_{i=0}^{n} B_{(i,n)}(t) x_i, \quad y(t) = \sum_{0}^{n} B_{(i,n)}(t) y_i. \tag{11}$$

There are two major issues in the Bézier curve. First, the curve is defined as an implicit curve $(x(t), y(t))$ based on t instead of an explicit function such as $y = f(x)$. Thus, we cannot directly estimate the energy value (function of $y(t)$) for any intermediate force value (function of $x(t)$). Because the difference between x_i points obtained from experiment is not uniform, $x(t)$ is not the first order polynomial. Subfigs. 2(a) and (b) show the Bézier curve for $x(t)$ and $y(t)$, respectively. Second, the curve is only guaranteed to pass the initial and terminal points at $t = 0$ and 1, respectively. Thus, the other points may not be included in the curve even though they are closely located.

To address these issues, we consider an *inverse Bézier* method to estimate an intermediate power value ($y(t)$) for any given force value ($x(t)$). We modify the $x(t)$ as the first order polynomial and calculate the proper value of t to obtain the corresponding $y(t)$. Then we can create a polynomial with degree of n,

$$x(t) = \sum_{i=0}^{n} B_{(i,n)}(t) c_i, \quad y(t) = \sum_{i=0}^{n} B_{(i,n)}(t) d_i, \tag{12}$$

where the curve passes $n + 1$ control points for given t_i ($i = 0, \cdots n$) from the 2-dimensional data set, $\{(x_i, y_i)\}_{i=0}^{n}$. The rationale behind this is to define both coefficients c_is and d_is to control the curve to pass the given data points. Thus, it can help our approximation, which is different from the Bézier method.

In this inverse Bézier method, we first make the $x(t)$ proportional to t. Because the $x(t)$ is now a straight line, we can construct an explicit inverse function as an inverse function of $x(t)$ for t_p from given x_p. Since the inverse function of the straight line, which has nonzero slope, is an another straight line, we have the inverse function t as a function of x,

$$t(x) = mx + t(0),$$

where m is a slope. Since the curve is forced to pass each data point ((x_i, y_i)) on given time (t_i), we can find a proper $y(t_p)$ from any value from t_p. From the 2-dimensional data set, $\{(x_i, y_i)\}_{i=0}^{n}$, each data point is to find the proper coefficient set, $\{c_i\}_{i=0}^{n}$ and $\{d_i\}_{i=0}^{n}$. Here, we define $c_0 = x_0$, $c_n = x_n$, $d_0 = y_0$, and $d_n = y_n$ because the curve should pass (x_0, y_0) and (x_n, y_n) at $t = 0$ and $t = 1$, respectively, as defined in Bézier method. Thus, we consider our explicit function for remaining $n - 1$ data points to define (c_i, d_i), where $i =$

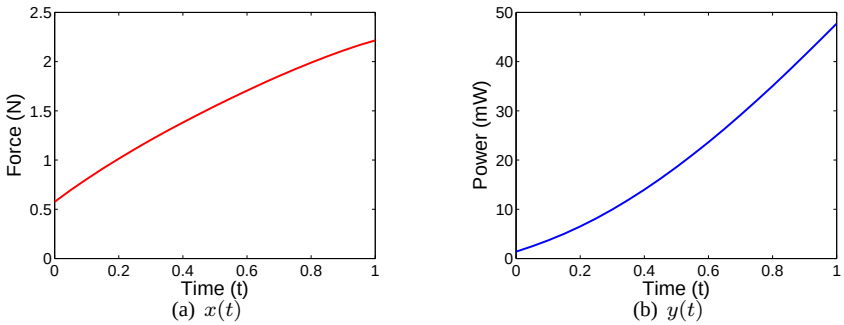

(a) $x(t)$ (b) $y(t)$

Fig. 2. The Bézier curve.

$$\begin{bmatrix} x_1 - (1-t_1)^n x_0 - t_1^n x_n \\ \vdots \\ x_{n-1} - (1-t_{n-1})^n x_0 - t_{n-1}^n x_n \end{bmatrix} = \begin{bmatrix} \frac{n!}{1!(n-1)!} t_1(1-t_1)^{n-1} & \cdots & \frac{n!}{(n-1)!1!} t_1^{n-1}(1-t_1) \\ \vdots & \ddots & \vdots \\ \frac{n!}{1!(n-1)!} t_{n-1}(1-t_{n-1})^{n-1} & \cdots & \frac{n!}{(n-1)!1!}\ t_{n-1}^{n-1}(1-t_{n-1}) \end{bmatrix} \begin{bmatrix} c_1 \\ \vdots \\ c_n \end{bmatrix} \quad (13)$$

$$\begin{bmatrix} y_1 - (1-t_1)^n y_0 - t_1^n y_n \\ \vdots \\ y_{n-1} - (1-t_{n-1})^n y_0 - t_{n-1}^n y_n \end{bmatrix} = \begin{bmatrix} \frac{n!}{1!(n-1)!} t_1(1-t_1)^{n-1} & \cdots & \frac{n!}{(n-1)!1!} t_1^{n-1}(1-t_1) \\ \vdots & \ddots & \vdots \\ \frac{n!}{1!(n-1)!} t_{n-1}(1-t_{n-1})^{n-1} & \cdots & \frac{n!}{(n-1)!1!}\ t_{n-1}^{n-1}(1-t_{n-1}) \end{bmatrix} \begin{bmatrix} d_1 \\ \vdots \\ d_n \end{bmatrix} \quad (14)$$

$1, \cdots, n-1$. For this, we provide the formula in Eqs. 13 and 14 to express x and y variables, respectively.

Based on the Eqs. 13 and 14, the formulas for x and y variables can be reduced to a matrix problem,

$$[p_x, p_y] = A\,[c, d]\,, \quad (15)$$

where p_x and p_y are the defined values from given data set. Also A is induced from the Bézier method, and c and d are the coefficient of designated polynomial coefficients of $x(t)$ and $y(t)$ variables. Note that since the formulas share the matrix A, we can prove that this $n-1$ by $n-1$ matrix is invertible, if $t_i \neq t_j$, $i \neq j$, $t_i \neq 1$, and $t_i \neq 0$. In this paper, we do not include the proof for its invertibility due to the page limitation. Thus, we can calculate the proper c_i $(i = 1, \cdots, n-1)$ by inverting the Eq. 15,

$$[c, d] = A^{-1}\,[p_x, p_y]\,. \quad (16)$$

Here, c_0 and c_n are already given. Then we can create a new curve for $x(t)$ by finding the proper t_p from $x(t)$ to estimate $y(t_p)$. For this, we make $x(t)$ the straight line on t and x variables. It is accomplished to define t_i values as the proportional to x_i values. Similarly, we can find d_i $(i = 1, \cdots, n-1)$. In Subfig. 3(a), $x(t)$ function shows a straight line and thus, the proper t_p value can be obtained by the corresponding $y(t_p)$. However, when t_p becomes small, the $y(t_p)$ values are significantly fluctuated and deteriorated due to its high order polynomial form.

In order to eliminate the fluctuation but keep the original structure of Bézier method, in this paper, we modify this inverse Bézier method by inserting a limited number of virtual data set in small t_p. Then we manage the curve to generate plausible $y(t_p)$ values. The rationale behind this is to generate a simple interpolation function, where the curve must pass the given data points. Thus, we can find the proper t_p for designated x_p value to obtain the corresponding $y(t_p)$ shown in Subfigs. 3(b) and (c).

In summary, we present a Bézier curve based interpolation function for a seamless energy conversion. In order to build an explicit interpolation function, we use an inverse Bézier method, which is further refined by the modified inverse Bézier method. The proposed interpolation function generates a smooth and close enough curve to the original data set with less computational complexity and overhead.

V. Numerical Results

To examine the proposed techniques, we not only use the Matlab for mathematical analysis but also develop a customized discrete-event driven simulator using CSIM [23] for performance evaluation. We use a 200 × 200 (m^2) rectangular network area, where 441 nodes are located in a grid topology (21 × 21 nodes). The impact arrival rate follows the Poisson distribution with a rate of λ, and the impact force is uniformly selected between 0.5 and 2.5 (N) values based on the PFCB-W14. To gain a realistic impact force, we scale the distance (D) down to 0.001 times and set the proportionality factor (κ) as 0.1.

First, we evaluate a single source of impact. We assume that the impact is occurred in the center of area with the maximum force. Then we observe the spread of impact based on the diffusion equation addressed in section III. In Subfigs. 4(a), (b), and (c), after the single source of impact, we show the corresponding forces in each node after 1, 3, and 9 seconds, respectively. According to the Eq. 7, the impact is spread to

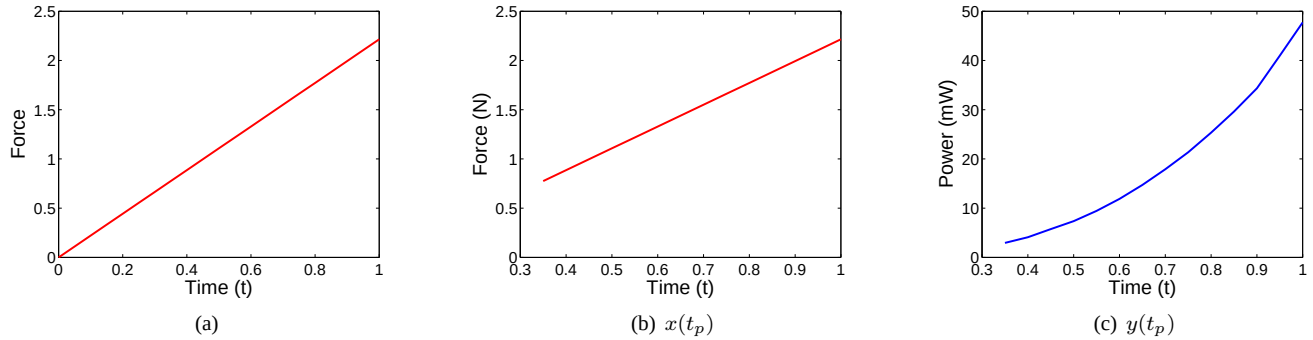

(a) (b) $x(t_p)$ (c) $y(t_p)$

Fig. 3. The inverse Bézier curve in terms of function $x(t)$ in (a), and its modified inverse Bézier curve in (b) and (c).

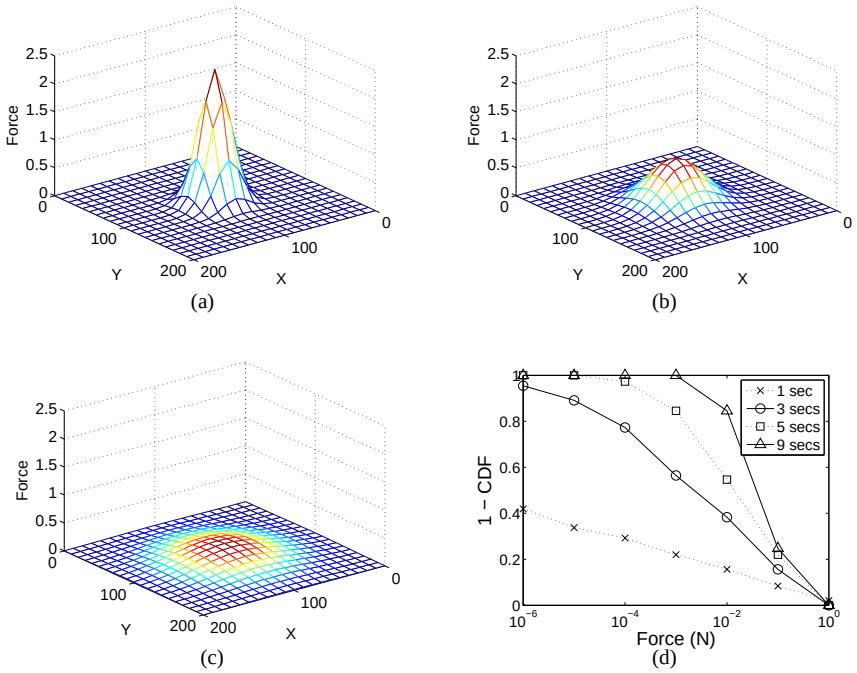

Fig. 4. The spreads of impact after single source of impact over time in (a), (b), and (c), and their cumulative force values in (d).

the nodes located in far away from the impact source with a very small force. Based on the impact spread after 1, 3, 5, and 9 seconds, Subfig. 4(d) shows the number of nodes that has the corresponding force and its cumulative statistics. After the impact, the force is rapidly reduced as the time increases and thus, most of the nodes have small force that has little effect to the piezoelectric device to generate an electrical energy.

Second, we examine the multiple sources of impact, in which each node is affected by prior impacts and its corresponding force is accumulated. In Fig. 5, we assume that three impacts are occurred consecutively with 2 seconds gap and their impact forces are randomly chosen. We also setup the impact locations at (50, 50), (100, 100), and (150, 150), respectively, to clearly see the influence of impacts in each node. As we have seen in the single impact, each impact force is rapidly reduced and distributed to adjacent nodes. Based on the sum of previous impact forces, each node converts it into an electrical energy.

Third, we evaluate the proposed interpolation function as a function of impact force. In Figure 6, we compare our approach with both curves derived from the original data set with PFCB-W14 and the Bézier technique. In contrast to the Bézier curve, which does not necessarily pass to the original data points except begin and end points, our curve based on the modified inverse Bézier technique passes the original data points for entire impact forces. Thus, the proposed interpolation function can find the reasonable intermediate data set based on the limited number of original data set.

VI. Concluding Remarks and Future Work

In this paper, we explored vibration-based energy harvesting techniques in WSNs. In order to characterize the vibration-

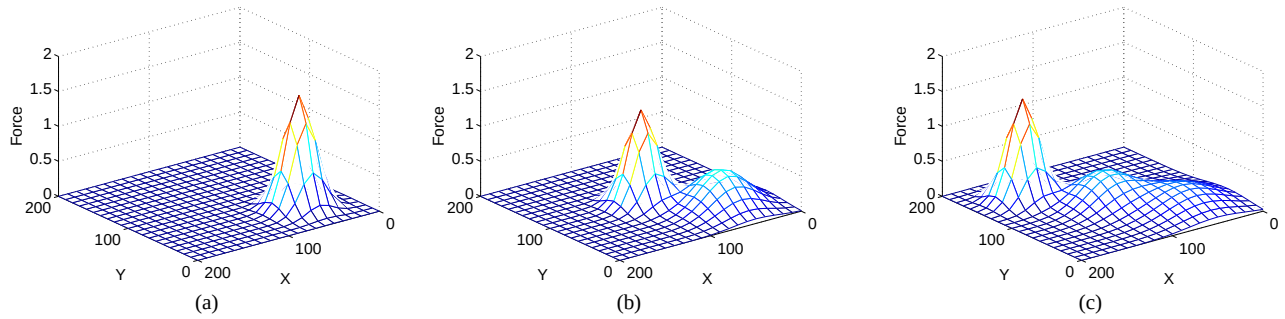

Fig. 5. The spreads of impact after multiple sources of impact over time.

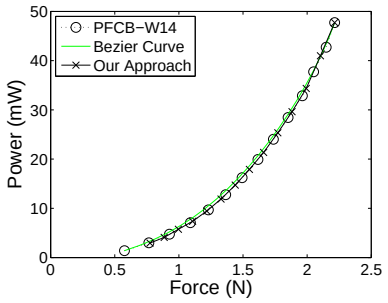

Fig. 6. Comparison between the Bézier curve and our approach in the presence of a limited number of original data set obtained by PFCB-W14.

motivated WSNs, we developed a simple model of impact spread and an interpolation function. We conducted a mathematical analysis and a simulation based performance study, and showed that the proposed techniques are proven to be a viable approach for analyzing vibration-motivated WSNs.

Although the low computational complexity and overhead is our primary concern, we plan to consider more rigorous mathematical approaches for explicit formulas as a future work. Also we plan to develop a energy harvesting aware routing protocol for vibration-motivated WSNs to exploit the full potential of the proposed techniques.

ACKNOWLEDGMENT

This research was supported in part by the Startup Grant in Dept. of Computer Science at Texas Tech University, US National Science Foundation (CNS-0831673 and CNS-1004210), and Advanced Cerametrics, Inc. (Lambertville, NJ 08530) for hardware support and technical advice.

REFERENCES

[1] I. F. Akyildiz, W. Su, Y. Sankarasubramaniam, and E. Cayirci, "A Survey on Sensor Networks," *IEEE Communications Magazine*, pp. 102–114, August 2002.

[2] S. Kim, S. Pakzad, D. Culler, J. Demmel, G. Fenves, S. Glaser, and M. Turon, "Health Monitoring of Civil Infrastructures Using Wireless Sensor Networks," in *Proc. IPSN*, 2007, pp. 254–263.

[3] K. Chebrolu, B. Raman, N. Mishra, P. K. Valiveti, and R. Kumar, "BriMon: A Sensor Network System for Railway Bridge Monitoring," in *Proc. Sensys*, 2008, pp. 2–14.

[4] H. Kim, S. Priya, H. Stephanou, and K. Uchino, "Consideration of Impedance Matching Techniques for Efficient Piezoelectri Energy Harvesting," *IEEE Trans. on Ultrasonics, Ferroelectrics, and Frequency Control*, vol. 54, no. 9, pp. 1851–1859, 2007.

[5] E. Hauseler, L. Stein, and G. Harbauer, "Implantable Physiological Power Supply with PVDF Film," *Ferroelectrics*, vol. 60, pp. 277–282, 1984.

[6] T. Starner, "Human-powered Wearable Computing," *IBM Systems Journal*, vol. 35, no. 3 & 4, pp. 618–629, 1996.

[7] L. M. Swallow, J. K. Luo, E. Siores, I. Patel, and D. Dodds, "A Piezoelectric Fibre Composite based Energy Harvesting Device for Potential Wearable Applications," *Measurement Science and Technology*, pp. 1–7, 2008.

[8] G. W. Taylor, J. R. Burns, S. M. Kammann, W. B. Powers, and T. R. Welsh, "The Energy Harvesting Eel: A Small Subsurface Ocean/River Power Generator," *IEEE of Oceanic Engineering*, vol. 26, no. 4, pp. 539–547, 2001.

[9] N. Xu, S. Rangwala, K. K. Chintalapudi, D. Ganesan, A. Broad, r. Govindan, and D. Estrin, "A Wireless Sensor Network for Structural Monitoring," in *Proc. Sensys*, 2004, pp. 13–24.

[10] T. Voigt, H. Ritter, and J. Schiller, "Utilizing Solar Power in Wireless Sensor Networks," in *Proc. IEEE LCN*, 2003, pp. 416–422.

[11] A. Kansal, D. Potter, and M. B. Srivastava, "Performance Aware Tasking for Environmentally Powered Sensor Networks," in *Proc. ACM SIGMETRICS/Performance*, 2004, pp. 223–234.

[12] K. Kar, A. Krishnamurthy, and N. Jaggi, "Dynamic Node Activation in Networks of Rechargeable Sensors," in *Proc. IEEE INFOCOM*, 2005, pp. 15–26.

[13] L. Lin, N. B. Shroff, and R. Srikant, "Asymptotically Optimal Power-Aware Routing for Multihop Wireless Wireless Networks with Renewable Energy Sources," in *Proc. IEEE INFOCOM*, 2005, pp. 1262–1272.

[14] A. Kansal, J. Hsu, M. Srivastava, and V. Raghunathan, "Harvesting Aware Power Management for Sensor Networks," in *Proc. DAC*, 2006, pp. 651–656.

[15] K. Zeng, K. Ren, W. Lou, and P. J. Moran, "Energy Aware Geographic Routing in Lossy Wireless Sensor Networks with Environmental Energy Supply," in *Proc. Quality of Service in Heterogeneous Wired/Wireless Networks*, 2006.

[16] M. Stordeur and I. Stark, "Low Power Thermoelectric Generator - Self-sufficient Energy Supply for Micro Systems," in *Proc. 16th Int'l Conf. on Thermoelectrics*, 1997, pp. 575–577.

[17] V. Raghunathan, A. Kansal, J. Hsu, J. Friedman, and M. Srivastava, "Design Considerations for Solar Energy Harvesting Wireless Embedded Systems," in *Proc. IPSN*, 2005, pp. 457–462.

[18] S. S. Nathan and P. A. Joseph, "Energy Scavenging with Shoe-Mounted Piezoelectrics," *IEEE Micro*, vol. 21, no. 3, pp. 30–42, 2001.

[19] J. Fritz, *Partial Differential Equations*. Springer-Verlag, 1991.

[20] S. A. Walter, *Partial Differential Equations: an Introduction*. John Wiley & Sons, 2008.

[21] A. J. Moulson and J. M. Herbert, *Electroceramics*. Cambridge, University Press, 1990.

[22] W. Cheney and D. Kincaid, *Numerical Mathematics and Computing*, 6^{th} *edition*. Thomson Brooks/Cole, 2008.

[23] *The CSIM User Guides*, http://www.mesquite.com/documentation.